

Charge-transfer range for photoexcitations in conjugated polymer/fullerene bilayers and blends

Dan Vacar

Institute for Polymers and Organic Solids, University of California, Santa Barbara, California 93106

Eric S. Maniloff and Duncan W. McBranch

Chemical Science and Technology Division, Mail Stop J585, Los Alamos National Laboratory, Los Alamos, New Mexico 87545

Alan J. Heeger

Institute for Polymers and Organic Solids, University of California, Santa Barbara, California 93106

(Received 17 March 1997)

Time-resolved photoinduced absorption was measured on bilayers of poly-[2-methoxy,5-(2'-ethylhexoxy)-1,4-phenylenevinylene] (MEH-PPV) and fullerene (C_{60}), and on MEH-PPV/ C_{60} composite films of various concentrations. We find that even in the picosecond regime, charge transfer from the conjugated polymer to C_{60} slows down the decay dynamics relative to the decay in the pure samples. The fact that charge transfer occurs in the picosecond time scale in bilayer structure (thickness ≈ 200 Å) implies that diffusion of localized excitations to the interface is not the dominant mechanism; the charge-transfer range is a significant fraction of the film thickness. From an analysis of the excited-state decay curves, we estimate the charge-transfer range to be 80 Å and interpret that range as resulting from quantum delocalization of the photoexcitations. [S0163-1829(97)04332-4]

I. INTRODUCTION

The nature of the primary photoexcitations in conjugated polymers such as poly(*p*-phenylene vinylene) (PPV) and its soluble derivatives remains an important and controversial issue. A fundamental question concerns the magnitude of the binding energy of the polaron excitation, i.e., what is the binding energy between positively and negatively charged polarons in semiconducting polymers? One can formulate the same question in terms of the spatial extent of the primary excitations: Is the wave function confined to a few repeated units of the conjugated polymer chain or is it extended over many monomers of the polymer backbone or even extended over multiple chains? Unfortunately, there is not yet a widely accepted answer. Data have been interpreted in terms of models that describe delocalized carriers with small exciton binding energies (0.1–0.2 eV or less) and spatial delocalization over 30 Å or more.¹ Alternatively, strongly correlated models have been proposed with exciton binding energies from 0.4 eV to greater than 1 eV,^{2,3} implying primary excitations with wave functions localized on the order of a single repeated unit. To resolve this issue, it is important to develop alternative methods of experimentally determining the spatial extent of excitations in conjugated polymers. These data will aid in developing theoretical models that can accurately describe the electronic properties of conjugated polymers in the solid state.

A number of previous experiments have studied the quenching of luminescence in conjugated polymer using nanosecond time-resolved or cw (non-time-resolved) luminescence measurements and applied these results to infer a diffusion range for excitons to defects that act as quenching sites. In one class of experiments⁴ pristine polymer samples were photo-oxidized in a controlled way to create a variable density of defects on the polymer chains. These defects are

formed photochemically in PPV when vinylene linkages are severed to form carbonyl species, which act as electron acceptors and efficient luminescence quenching sites. A diffusion time of order 1 ns was estimated and a corresponding diffusion range of 50 Å was inferred. In a second class of experiments, exciton dissociation properties were inferred from steady-state experiments of bilayer structures comprised of PPV/ C_{60} (Ref. 5) and PPV oligomer/Ca.⁶ Dissociation occurs at the interface because the electron and hole are separated by charge transfer. Diffusion ranges of 70 and 200 Å respectively, were inferred.

The C_{60} molecules in the polymer/fullerene mixtures are in some ways analogous to the defect sites in the photooxidized polymer system described above.^{4,7} After photoexcitation, the electron in the π^* band transfers from the polymer (as the donor) to the C_{60} (as the acceptor).⁸ With the addition of a few percent C_{60} , luminescence is quenched by approximately three orders of magnitude, relative to the pure conjugated polymer. The quenching results from charge transfer, which separates the electron and the hole on a time scale three orders of magnitude faster than the radiative decay time. The implied forward electron transfer rate indicates that charge transfer occurs in the picosecond time scale:

$$\frac{1}{\tau_{CT}} = \left(\frac{1}{Q} \right) \left(\frac{1}{\tau_{rad}} \right) \geq 10^3 \times 10^9 > 10^{12} \text{ s}^{-1}, \quad (1)$$

where $1/\tau_{CT}$ is the charge-transfer rate, $1/\tau_{rad}$ is the radiative lifetime, and $Q \ll 1$ is the quenching ratio. Measurements of photoinduced absorption and photoinduced dichroism showed that in the polymer/fullerene system charge transfer occurs within a few hundred femtoseconds,⁹ in agreement with Eq. (1).

The ultrafast charge-transfer process has been challenged recently.¹⁰ A forward charge-transfer time of more than 10

ps was inferred from transient absorption studies on a heavily doped PPV-derivative/ C_{60} blend. In the present work a larger range of concentrations, as well as charge transfer at a donor/acceptor interface, has been studied in an attempt to resolve this controversy. Even in relatively thick bilayer structures, we observe the effects of charge transfer in the picosecond regime. We develop a quantitative model that describes the ultrafast nature of the charge transfer process in MEH-PPV/ C_{60} composites and bilayers. The change in dynamics during the first few picoseconds results from charge transfer occurring in parallel with exciton-exciton bimolecular recombination. The dynamics of photoinduced charge transfer can be used to infer a spatial extent of the excitons on time scales too short for diffusion to play a significant role. We show that the dynamical data imply a delocalization of the excitonic wave function in MEH-PPV over approximately 80 \AA . Diffusion across this distance in less than 1 ps is eliminated as a possibility. Delocalization over such distances implies that the exciton binding energy must be relatively small.

II. EXPERIMENT

A. Sample preparation

The MEH-PPV/ C_{60} blends were spin cast at 1500 rpm to obtain 2000-\AA -thick films [the optical density (OD) equals 2 at peak absorption]. Blends having three concentrations of the acceptor molecule were prepared: 5 wt. % (2 mol %), 10 wt. % (4 mol %), and 25 wt. % (10 mol %). Visual examination showed that the films were of excellent optical quality.

For bilayers, MEH-PPV films were first spin cast from dilute solutions onto sapphire substrates, followed by evaporation of a 400-\AA layer of C_{60} . A 200-\AA layer (measured with Dektak profilometer) was cast at 4000 rpm (the measured OD for the polymer layer was 0.2 at maximum absorption).

B. Instrumentation for transient absorption

The second harmonic of a regeneratively amplified Ti:sapphire laser (Clark-MXR CPA 1000) provided a 400-nm (3.1-eV) pump pulse (150-fs pulse width). At this wavelength (on the high-energy side of the absorption maximum), the polymer absorbs strongly, while the absorption from C_{60} is much smaller. Therefore, the C_{60} molecules are not excited directly by the pump in significant quantity. The pump energy was approximately $3 \mu\text{J}$ per pulse illuminating an area of 1 m^2 at the sample plane. The intensity of the pump beam was varied using neutral density filters. The photoexcited sample was then probed in the near-IR with the 800-nm (1.55-eV) fundamental beam.

The probe was time delayed with respect to the pump by passing the probe beam through a computer controlled delay stage before reaching the sample. The pump beam was mechanically chopped and phase sensitive (lock-in) detection was utilized to detect the modulation in the transmitted probe intensity. During the measurements on the bilayer structure, the pump and the probe beams were incident on the C_{60} layer and reached the polymer through the C_{60} /polymer interface. The samples were kept in vacuum to avoid photo-oxidation. All measurements were performed with samples at room temperature.

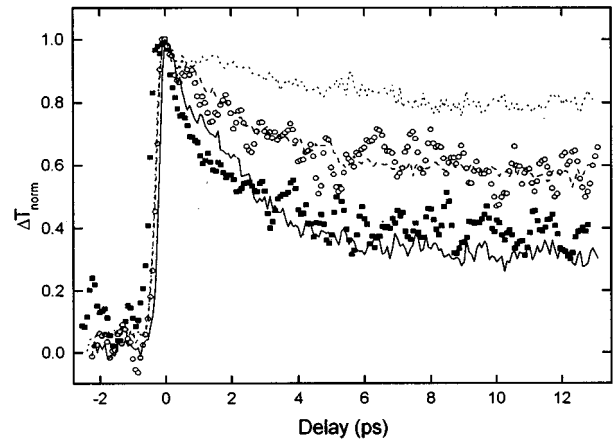


FIG. 1. Decay dynamics for MEH-PPV/ C_{60} blends: 0 wt. %, solid line; 5 wt. %, dashed line; and 25 wt. %, dotted line, for a thin (200-\AA) MEH-PPV monolayer, squares, and a (200-\AA) MEH-PPV/ C_{60} bilayer, circles.

III. RESULTS

The 400-nm pump pulse caused a reduction in the transmitted intensity of the 800-nm probe pulse (photoinduced absorption). The relative change in transmission $\Delta T/T$ is directly proportional to the change in absorption $\Delta\alpha$, where $\Delta\alpha = \sigma N$, with σ the excited-state absorption cross section and N the excited-state population density. The photoinduced absorption decreases with time as a consequence of the decay of the excited-state population.

Transient photoinduced absorption data obtained at 800 nm from MEH-PPV/ C_{60} bilayers and blends are presented in Fig. 1. The incident excitation density for all data in Fig. 1 was $N_0 = 2.5 \times 10^{19} \text{ cm}^{-3}$. The population decay in the blends (solid lines) slows down as the acceptor concentration increases from the pure sample to the 5 wt. % blend and then to the 25 wt. % blend. The results for the bilayer structures correspond to the thinnest MEH-PPV film that we could prepare. Two other films produced data that were identical, within the experimental resolution, to the data presented here. A reasonably good overlap of the normalized decay curves of the pure MEH-PPV samples (thin and thick samples) is observed in Fig. 1. Small differences result from the different substrates and the different thickness of the two samples (see Ref. 2).

Three experimental facts emerge from Fig. 1. (i) The presence of C_{60} in the vicinity of the polymer (at the interface in bilayers or intermixed blends) slows down the decay dynamics relative to the decay in the pure samples. As a consequence of the charge transfer, the excited state of the polymer/ C_{60} system is longer lived than the excited state of the pristine parent polymer. (ii) The quenching of the fast component decay is evident on picosecond time scales, indicating ultrafast charge transfer in bilayer structures (thickness $\approx 200 \text{ \AA}$). (iii) The decay dynamics of the polymer/fullerene bilayer system (MEH-PPV) thickness $\approx 200 \text{ \AA}$ (circles) is essentially identical to the decay dynamics of the 5 wt. % homogeneous blend. With these experimental observations in mind, we turn to a discussion of the nature of the excited state and the decay mechanism that leads to the measured photoinduced absorption (PA) data.

IV. DISCUSSION

Diffusion of localized excitations to the interface cannot explain the observation of charge transfer in bilayers within the picosecond regime. The diffusion length over a distance d can be expressed as

$$d^2 = Dt, \quad (2)$$

where D is the diffusion coefficient and t is the time. Assuming $d \approx 100$ Å for the bilayers and $t \approx 10^{-12}$ s, D would be of order 1 cm²/s. Using Einstein's relation $\mu = eD/k_B T$, where μ is the mobility, e is the electron charge, k_B is the Boltzmann constant, and T is the temperature, we conclude that $\mu \approx 40$ cm²/V s would be required. Such large diffusion constants (and mobilities) are not possible either for charged polarons or for neutral excitons in disordered polymers: From picosecond transient photoconductivity measurements, the charge carrier (polaron) mobility in semiconducting polymers has been estimated to be¹¹ 0.5 cm²/V s. Under steady-state conditions, the carrier mobility is much smaller. $D = 2 \times 10^{-4}$ cm² s⁻¹ was estimated for PPV in the nanosecond quenching experiments⁴ mentioned above. Neutral exciton diffusion constants are only of order 10^{-5} – 10^{-4} cm² s⁻¹ even in organic single crystals.¹² Therefore, in order to explain the rapid charge transfer over such long distances, the wave functions of the primary excitations must be spatially extended over distances approaching 100 Å. In the remainder of this section, we present a detailed analysis of the decay that enables a quantitative estimate of the charge-transfer range.

There has been a considerable volume of recent work^{4,13–15} concerning the nature of the excited-state species in conjugated polymers and in particular which species contribute to the near-IR PA band around 800 nm. For simplicity we will assign the PA of pristine MEH-PPV at 800 nm to a single excited-state species. We denote the population of this excited state as N_{ex} . For the following discussion, the size of the exciton binding energy is not important. Moreover, it is not relevant whether the primary excitation is emissive or nonemissive.

A number of recent papers have discussed bimolecular annihilation processes in PPV derivatives.^{14,16,17} It was demonstrated that the intensity-dependent dynamics of the excited-state absorption in PPV oligomers can be modeled by a rate equation of the form¹⁴

$$\frac{dN_{\text{ex}}}{dt} = -\frac{N_{\text{ex}}}{\tau} - \frac{\beta}{\sqrt{t}} N_{\text{ex}}^2, \quad (3)$$

where the first term represents the natural lifetime decay and the second term describes the bimolecular arising from the interaction between excitations. At low excitation densities, the first term is dominant and the decay is exponential. At high excitation densities the second term is dominant at early times when the excited species annihilate.¹⁸ The fast initial decay rapidly leads to densities sufficiently low that the natural decay dynamics are recovered at later times. The excitation densities and the mean separation between excitations encountered in our experiment (see Ref. 2) fall within the regime where Eq. (1) applies reasonably well.

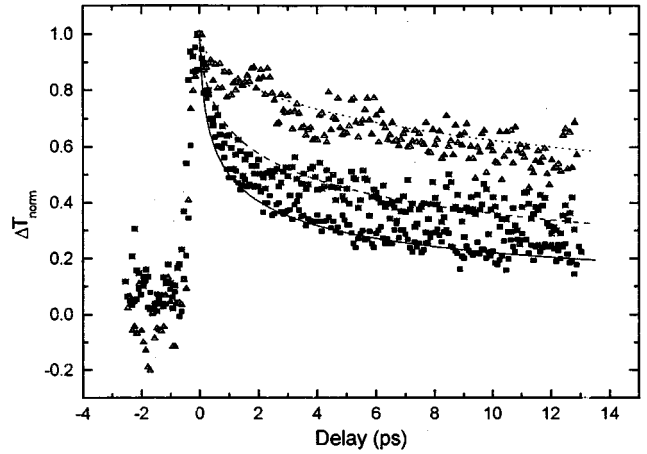


FIG. 2. Decay dynamics for MEH-PPV at various incident excitation densities: $N_0 = 5 \times 10^{19}$ cm⁻³, squares; $N_0 = 2.5 \times 10^{19}$ cm⁻³, circles; and $N_0 = 5 \times 10^{18}$ cm⁻³, triangles. The lines represent solutions to a bimolecular decay rate equation (see the text).

Bimolecular dynamics of the form shown in Eq. (3) (i.e., with the $t^{-1/2}$ factor) arise in three dimensions when the interaction between excitations arises from spatial delocalization rather than from particle diffusion.¹⁸ Particle diffusion in three dimensions gives a nonlinear component in the rate equation proportional to N_{ex}^2 (independent of time).¹⁸ Since the long-range nature of the charge transfer also implies three-dimensional (3D) interactions of the excitons and since the time scales for the bimolecular decay are again too rapid for diffusion to be important, we use the form as shown in Eq. (3), which only accounts for annihilation by wave function overlap in the 3D limit.

The early time decay dynamics for pristine MEH-PPV (the thick sample) are presented in Fig. 2. The parameters used to fit the data are the natural lifetime $\tau = 500$ ps and the bimolecular factor $\beta = 1.2 \times 10^{-20}$ cm³ ps^{-1/2}. As expected, the fast component of the population decay is reduced when the initial excitation density decreases. The quality of the fits implies that Eq. (3) (with the $t^{-1/2}$ factor) can provide a simple quantitative means to understand the intensity-dependent recombination dynamics in these materials, despite the fact that in Eq. (3) many features of decay in real samples are neglected (including nonexponential decay mechanisms at low excitation densities and also the variation of excitation density along the sample to absorption of the pump beam). This latter effect in the bilayers results in an excitation density at the rear of the sample approximately 0.6 times the value at the entrance face; in the bulk samples the variation along the sample is larger still. However, a more detailed model is not necessary to show the basic physical features that contribute to the decay in our samples.

In the presence of C₆₀, the excited-state absorption $\Delta\alpha$ arises from a superposition of the remaining primary excitations N_{ex} and the newly formed charge-transferred excitations N_{CT} :

$$\Delta\alpha(t, \lambda) = N_{\text{ex}}(t)\sigma_{\text{ex}}(\lambda) + N_{\text{CT}}(t)\sigma_{\text{CT}}(\lambda). \quad (4)$$

The spectral dependence of each excited species is determined by its cross section σ_i .

The physical model that describes the data follows the functional form of Eq. (4), with the following features. (i) The charge-transferred population N_{CT} is formed at times within the experimental resolution (approximately 200 fs).^{9,19} (ii) The magnitude of N_{CT} is approximately constant in the picosecond regime.

Equation (4) implies that the two components of the excited-state population are not strongly interacting. Feature (i) implies that by the time the pump beam leaves the sample, a population N_{CT} of charged-transferred states has formed, leaving behind a population $N_{ex} = N_0 - N_{CT}$ of primary states on the polymer chains. This reduced “initial” population of N_{ex} then decays via its intrinsic decay channels. Feature (ii) is valid because the forward and the reverse charge-transfer rates are highly asymmetric; while the forward charge transfer occurs on subpicosecond times, the lifetime for the charge-transferred state can be up to milliseconds.^{8,9} Thus, during the first 10 ps, the contribution of N_{CT} to $\Delta\alpha$ will be approximately constant.

We have shown that for pristine thin films of MEH-PPV the nonlinear decay of the primary excitations N_{ex} can be deduced from the intensity-dependent decay of $\Delta\alpha$ at 800 nm. In the bilayer, a fraction of N_{ex} transfers an electron to the C_{60} layer, thereby forming N_{CT} states within 1 ps. As a result, the bimolecular decay of the population N_{ex} slows down because the effective initial population is reduced relative to that when there is no C_{60} layer. In addition, the states N_{CT} contribute a near-constant component to the decay dynamics. The general effect is a concerted slowing down (“flattening”) of the PA decay. In the following, we use the parameters derived from the fits of the dynamics in the thin layers of MEH-PPV, together with the relative magnitude of $\Delta\alpha$ at 800 nm in the bilayer to deduce both the charge-transfer probability ξ and the relative excited-state cross section of the charge-transferred probability state σ_{CT}/σ_{ex} . To do this, we first normalize the measured $\Delta T/T$ curve in the bilayer to the value of the pristine thin film at a zero delay and we rewrite Eq. (4) in the form

$$\Delta T_{\text{norm}} = (1 - \xi)g(t, \xi) + \xi \frac{\sigma_{CT}}{\sigma_{ex}}. \quad (5)$$

The decay function $g(t, \xi)$ in the first term of Eq. (5) is simply the nonlinear decay obtained by integrating Eq. (2) with the same parameters τ and β used to fit the dynamics of the primary excitations N_{ex} in the pristine samples. The dependence of this decay function on ξ is included explicitly to indicate the sensitivity of the bimolecular decay to the percentage of states undergoing charge transfer, as described above. The second term accounts for the time-dependent contribution to $\Delta T/T$ from N_{CT} ; the correct magnitude for this second term is crucial to achieve the proper value of ΔT_{norm} at zero delay (0.82 in our measurement relative to the pristine thin film). The strength of the two components (found self-consistently) yields the relative fraction of the two species that contribute to the excited-state absorption at 800 nm.

As shown in Fig. 3, this simple self-consistent model yields excellent fits to the data. The fraction of charge-transferred states extracted from the fit is $\xi = 0.38 \pm 0.03$, with a value of $\sigma_{CT}/\sigma_{ex} = 0.53 \pm 0.04$. A corresponding fraction of

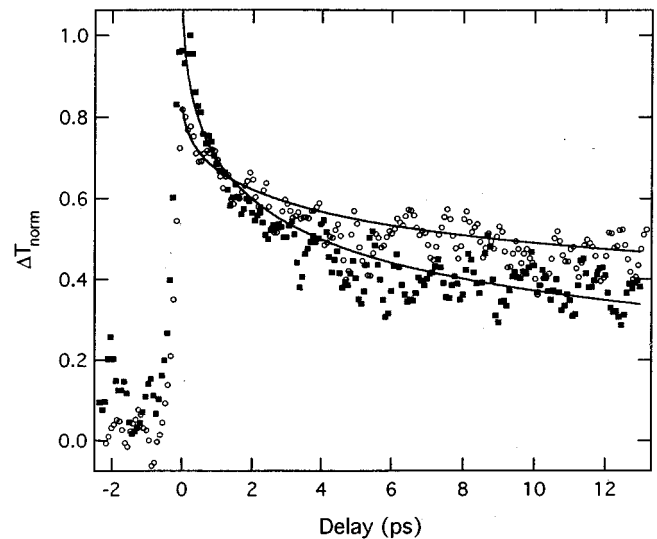


FIG. 3. Decay dynamics for thin (200-Å) MEH-PPV monolayer, squares, and a (200-Å) MEH-PPV/(400-Å) C_{60} bilayer, circles. The lines represent fits to a model involving bimolecular decay of primary excitations in the MEH-PPV and a constant contribution from long-lived charge-transferred states (see the text).

the polymer layer participates in the charge transfer. Therefore, we infer an effective charge-transfer range of approximately 80 Å from the fit in Fig. 3. This more accurate value is consistent with the qualitative conclusion, inferred from the observation that charge transfer occurs in the picosecond time scale in bilayer structures (thickness ≈ 200 Å), that the charge-transfer range is a significant fraction of the film thickness.

We showed in Fig. 1 that the PA dynamics for the bilayer and for the 5 wt. % blend are almost the same, implying a similar fraction of charge-transferred species in these two cases: about 40%. The obvious trend for the MEH-PPV/fullerene blends is that as the concentration of C_{60} increases, a larger fraction of the primary excitation population undergoes charge transfer in the first picosecond. However, even at high concentrations, the efficiency of charge transfer on picosecond time scales does not reach 100%. The high-concentration limit was studied by Kraabel *et al.*⁹ in transient PA measurements of 50 mol % functionalized fullerene/polymer blends. The data presented in Fig. 6 of Ref. 9 indicate that even at these high concentrations some decay is observed on the picosecond time scale; the intrinsic decay of on the order of 15% of the excitations remaining on the polymer accounts for this observed decay and implies that phase separation of the polymer/fullerene composite at high concentrations of fullerene is the limiting factor for complete charge transfer within the first picosecond. On longer time scales, of course, diffusion still plays a significant role in the charge-transfer process, especially for composites at lower fullerene concentrations. For example, we conclude that in the 5 wt. % bulk blend approximately 40% of the primary excitations undergo charge transfer in the first picosecond. However, the luminescence in these samples is quenched by more than three orders of magnitude, indicating that on time scales intermediate between the intrinsic forward transfer time and the radiative lifetime (10 ps–1 ns) the diffusion of

excitations to find acceptor sites is the dominant decay channel for the remaining excitations on the polymer.

V. SUMMARY AND CONCLUSIONS

Time-resolved photoinduced absorption experiments on MEH-PPV/C₆₀ bilayers and on composites of various concentrations showed that the presence of C₆₀ slows down the picosecond decay dynamics relative to the decay in the pure samples. As a consequence of the charge transfer, the excited state of the polymer/C₆₀ system is longer lived than the excited state of the pristine parent polymer. The fact that a large fraction of excited states undergo charge transfer in bilayer structures implies that the charge-transfer range is a significant fraction of the film thickness. This conclusion holds true regardless of the model used to interpret the data.

In order to obtain more quantitative results, a model was developed that assumes that the PA dynamics results from two noninteracting species, the primary excitations and the charge-transferred states. Charge transfer occurs in less than 1 ps. The primary excitations follow bimolecular decay dynamics, while the charge-transferred states are long lived. Based on this model we conclude that in the bilayers, 38(±3)% of the initial photoexcitations on the polymer undergo ultrafast charge transfer. A similar fraction of the initial photoexcitations are charge transferred in the 5 wt. % blends. The ratio of excited-state absorption cross sections of the charge-transferred state to the polymer excited state at 800 nm is $\sigma_{CT}/\sigma_{ex}=0.53\pm 0.04$. Diffusion of localized excitations to the interface cannot explain the observation of charge transfer in bilayers within the picosecond regime; the required diffusion constants for charged polarons or for neutral excitons would be too large by at least two orders of magnitude. In order to explain the rapid charge transfer over such long distances, the wave functions of the primary excitations must be spatially extended over approximately 80 Å.

McBranch *et al.* showed²⁰ that for thin films, spin cast at high rpm, the polymer chains are arranged primarily parallel to the substrate. In the bilayer structures, the MEH-PPV layer was thin (200 Å) and was spin cast at 4000 rpm, implying that the delocalization length estimated in this work is primarily transverse to the polymer chains. A quasi-three-dimensional wave function, extended over 80 Å for the primary excitations of the luminescent polymers, is in agreement with the 100-Å localization length found from studies of the metal-insulator transition in conducting polymers (polyaniline and polypyrrole).^{21,22}

The inferred spatial extent of the wave function of 80 Å is larger than the value of 30 Å (5 monomers) often quoted for PPV (Refs. 23 and 24) and would imply spatial delocalization over approximately 13 monomers. The persistence length for MEH-PPV has been estimated²⁵ to be 60 Å (in solution); this would be a lower bound for delocalized, weakly interacting polarons. The large spatial spread of the primary excitations inferred from the present measurements implies a weak binding energy between the charged polarons (“electrons and holes”), i.e., 0.05–0.1 eV, or a few times kT .

ACKNOWLEDGMENTS

We thank Jun Gao, Christian Heller, and Dr. Ian Campbell for assistance with the sample preparation. We benefited from discussion with Dr. Ben Schwartz, Kirk Miller, and Dr. Uli Lemmer. Work at UCSB was supported by the Air Force Office of Scientific Research (Dr. Charles Lee) under Grant No. F49620-96-1-0107 and by a grant from the Los Alamos National Laboratory–University of California Program, Grant No. STP/UC:96-136. Work at Los Alamos was also funded through the Laboratory Directed Research and Development Program, under the auspices of the U.S. Department of Energy.

-
- ¹J.-L. Bredas, J. Cornil, and A. J. Heeger, *Adv. Mater.* **8**, 447 (1996).
²J. M. Leng *et al.*, *Phys. Rev. Lett.* **72**, 156 (1994).
³M. Chandross *et al.*, *Phys. Rev. B* **55**, 1486 (1997).
⁴L. J. Rothberg *et al.*, *Synth. Met.* **80**, 41 (1996).
⁵J. M. Halls *et al.*, *Appl. Phys. Lett.* **68**, 3120 (1996).
⁶V. Choong *et al.*, *Appl. Phys. Lett.* **69**, 1492 (1996).
⁷N. T. Harrison *et al.*, *Phys. Rev. Lett.* **77**, 1881 (1996).
⁸N. S. Sariciftci *et al.*, *Science* **258**, 1474 (1992).
⁹B. Kraabel *et al.*, *J. Chem. Phys.* **104**, 4267 (1996).
¹⁰X. Wei, S. V. Frolov, and Z. V. Vardeny, *Synth. Met.* **78**, 295 (1996).
¹¹C. H. Lee *et al.*, *Phys. Rev. B* **49**, 2396 (1994).
¹²M. Pope and C. E. Swenberg, *Electronic Processes in Organic Crystals* (Clarendon, Oxford, 1982).
¹³B. J. Schwartz *et al.*, *Chem. Phys. Lett.* **265**, 327 (1997).
¹⁴E. S. Maniloff, V. Klimov, and D. McBranch, *Phys. Rev. B* **56**, 1876 (1997).
¹⁵D. McBranch and M. B. Sinclair, in *Nature of the Photoexcitations in Conjugated Polymers: Semiconductor Band vs Exciton Model*, edited by N. S. Sariciftci (World Scientific, New York, in press).
¹⁶R. G. Kepler *et al.*, *Synth. Met.* **78**, 227 (1996).
¹⁷G. J. Denton *et al.*, *Phys. Rev. Lett.* **78**, 733 (1997).
¹⁸R. C. Powell and Z. G. Soos, *J. Lumin.* **11**, 1 (1975).
¹⁹B. Kraabel *et al.*, *Phys. Rev. B* **50**, 18 543 (1994).
²⁰D. McBranch *et al.*, *Appl. Phys. Lett.* **66**, 1175 (1995).
²¹M. Reghu *et al.*, *Phys. Rev. B* **47**, 1758 (1993).
²²C. Yoon *et al.*, *Phys. Rev. B* **49**, 10 851 (1994).
²³D. Beljonne *et al.*, *J. Chem. Phys.* **102**, 2042 (1995).
²⁴J. Cornil, D. Beljonne, and J. L. Bredas, *J. Chem. Phys.* **103**, 842 (1995).
²⁵C. L. Gettinger *et al.*, *J. Chem. Phys.* **101**, 1673 (1994).